

# Glacial-interglacial changes in marine silicon isotopic distribution

Shuang Gao<sup>1,2</sup>, Dieter A. Wolf-Gladrow<sup>3</sup>, Christoph Völker<sup>3</sup> ([christoph.voelker@awi.de](mailto:christoph.voelker@awi.de))

1. Geophysical Institute, University of Bergen, Norway 2. Bjerknes Centre for Climate Research 3. Alfred-Wegener-Institut Helmholtz-Zentrum für Polar- und Meeresforschung, Germany

## Introduction

Reconstruction of silicic acid utilisation by diatoms in the Southern Ocean is of importance for understanding the ocean's role in controlling atmospheric CO<sub>2</sub> variations during glacial-interglacial cycles. The silicon stable isotopic composition ( $\delta^{30}\text{Si}$ ) of biogenic silica (BSi) is used as a proxy for silicic acid utilisation and marine Si cycling in the past. A Last Glacial Maximum (LGM) and a present-day (PD) climate simulation have been performed with a coupled ocean-sediment model including a prognostic formulation of BSi production with silicon isotopic fractionation. Our aim is to model variations of marine  $\delta^{30}\text{Si}$  in the last glacial-interglacial cycle, to reveal possible controlling mechanisms of the LGM  $\delta^{30}\text{Si}$  distribution, and to see whether these affect the interpretation of  $\delta^{30}\text{Si}$  as a proxy for silicic acid utilisation

## Model Setup

- Ocean Model:** Max-Planck-Institute global Ocean/Sea-Ice Model (MPI-OM)
- Biogeochemical Model:** Hamburg Ocean Carbon Cycle Model (HAMOCC5.1) with added Si isotopes
- Resolution:** horizontally 3°; vertically 40 layers
- Forcing:** from coupled atmosphere-ocean simulations under pre-industrial (the control run, PD) or LGM climate conditions (Zhang et al., 2013)
- Integration time:** 10,000 model years; annually averaged results of model year 10,000 are presented here

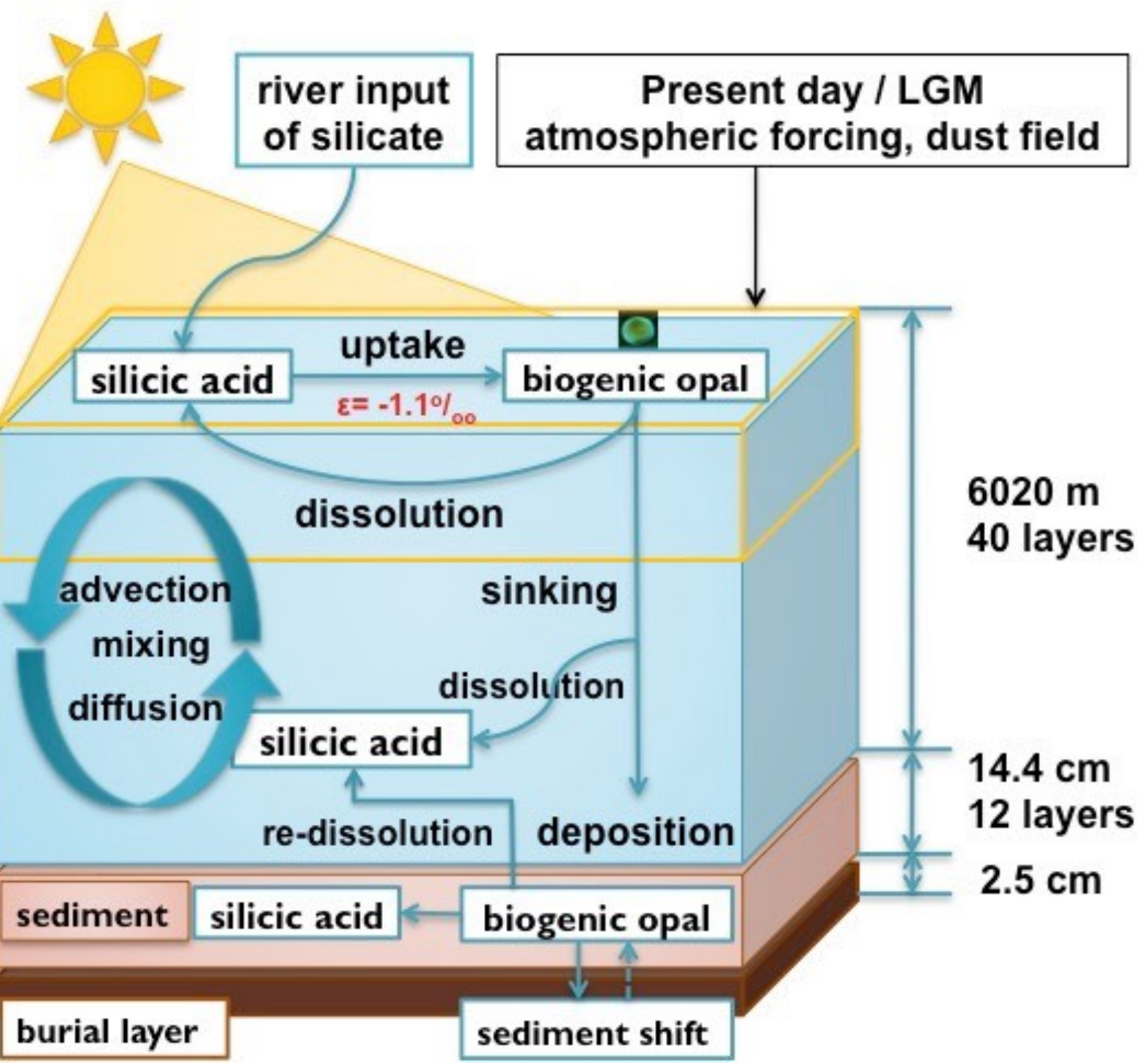


Figure 1: Schematic drawing of the silicon cycle in HAMOCC.

## Ocean physics

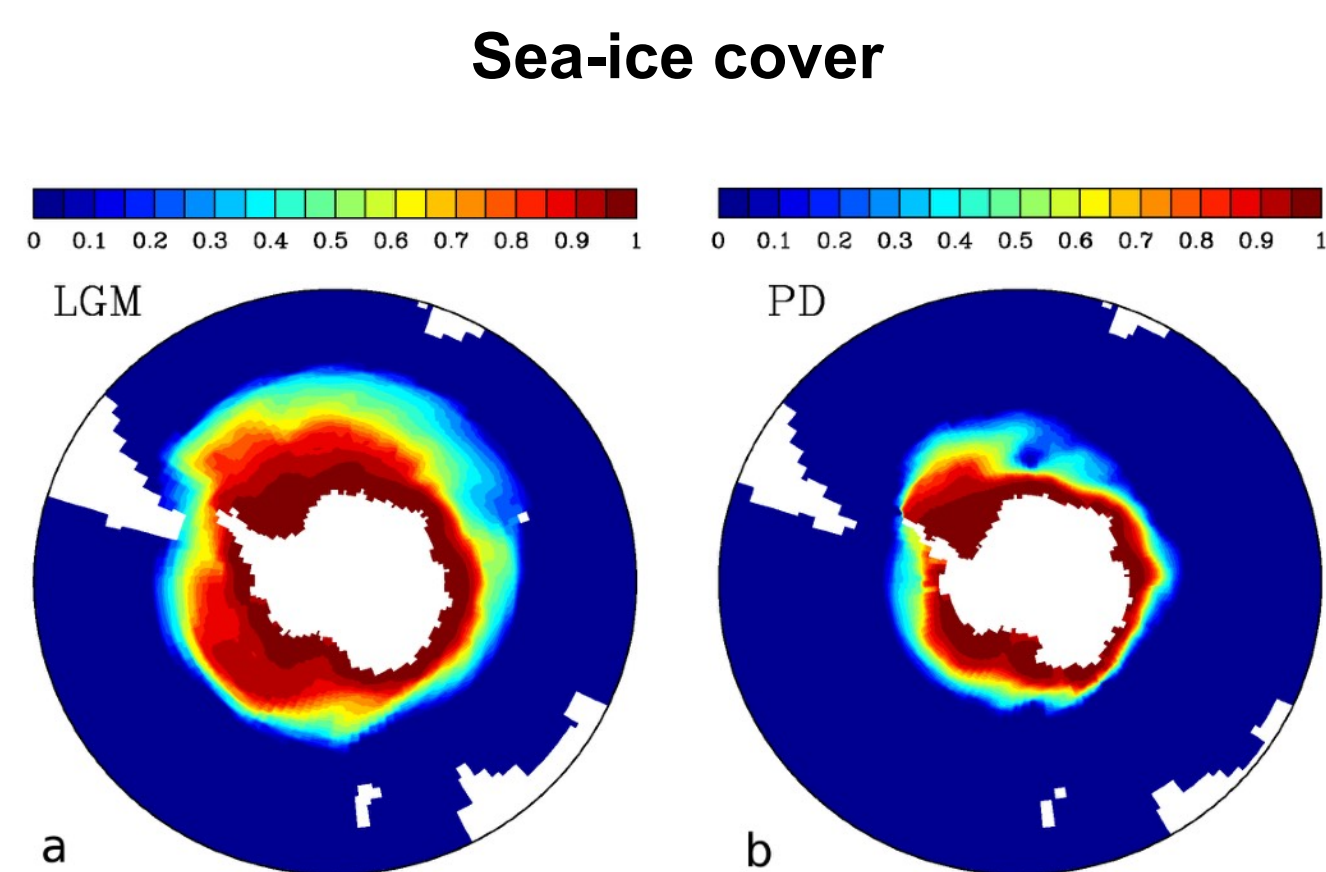


Figure 2: Annual mean fractional sea-ice cover in the Southern Hemisphere in the (a) LGM run and (b) PD run.

- Extended antarctic sea-ice cover during the LGM
- Shift to more extensive and more salty AABW in the Atlantic; less and shallower NADW

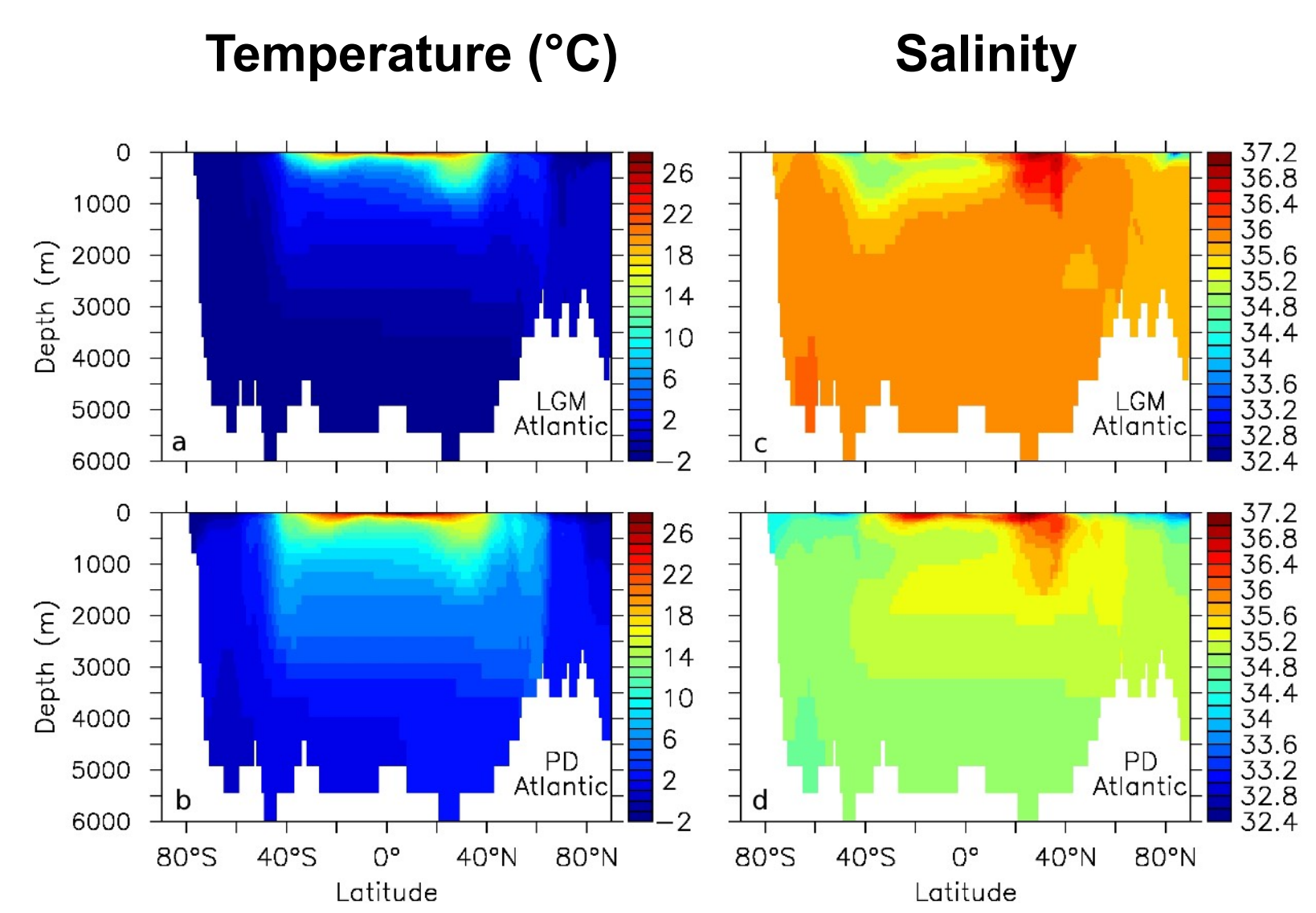


Figure 3: Zonal mean (a, b) temperature (°C) and (c, d) salinity in the Atlantic in the (a, c) LGM run and (b, d) PD run.

## Results and Discussion

### 1. Silicic acid distribution

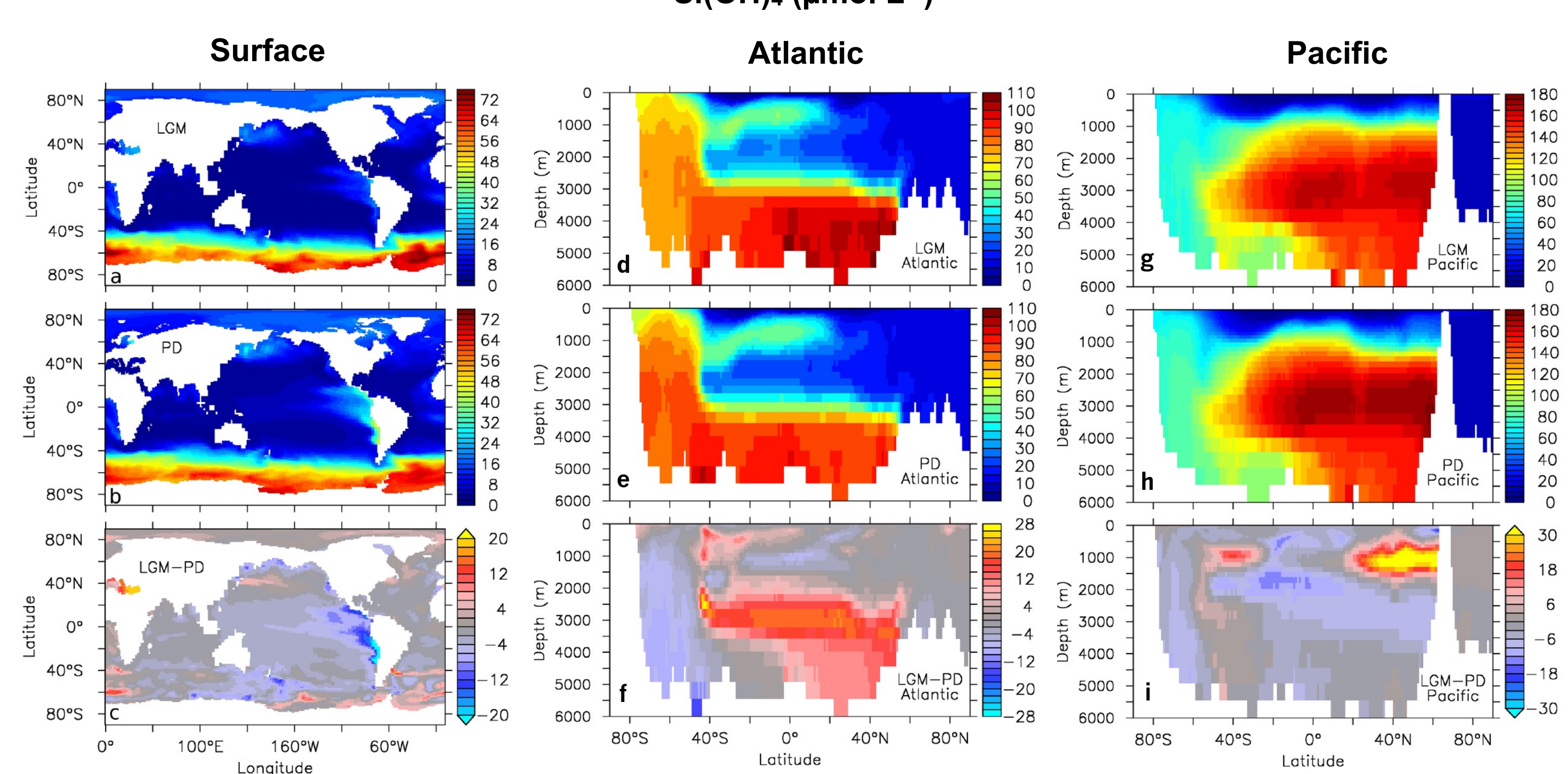


Figure 4: (a-c) Annual mean surface silicic acid concentrations ( $\mu\text{mol L}^{-1}$ ); (d-f) zonal average of silicic acid concentrations ( $\mu\text{mol L}^{-1}$ ) in the Atlantic and (g-i) in the Pacific. (a)(d)(g) the LGM run, (b)(e)(h) the PD run, (c)(f)(i) difference between the LGM and PD runs.

- Extended sea-ice cover in the Antarctic during the LGM causing reduction and northward shift of phytoplankton growth, and excess silicic acid being transported by Subantarctic Mode Water (SAMW) and Antarctic Intermediate Water (AAIW) to lower latitudes.
- Shift in silicic acid concentration from the deep Pacific to the North Atlantic, corresponding to shallower NADW and more extensive AABW in the Atlantic.

### 2. The $\delta^{30}\text{Si}$ distribution

- The global mean  $\delta^{30}\text{Si}_{\text{DSi}}$  in the upper ocean is 0.14‰ lower in the LGM run.
- The higher values in the subtropical gyres in the LGM run are shifted equator-ward likely due to ice extension in high latitudes.
- Global average vertical profiles of the LGM run are shifted toward lower values of both  $\delta^{30}\text{Si}_{\text{DSi}}$  and  $\delta^{30}\text{Si}_{\text{BSi}}$ .

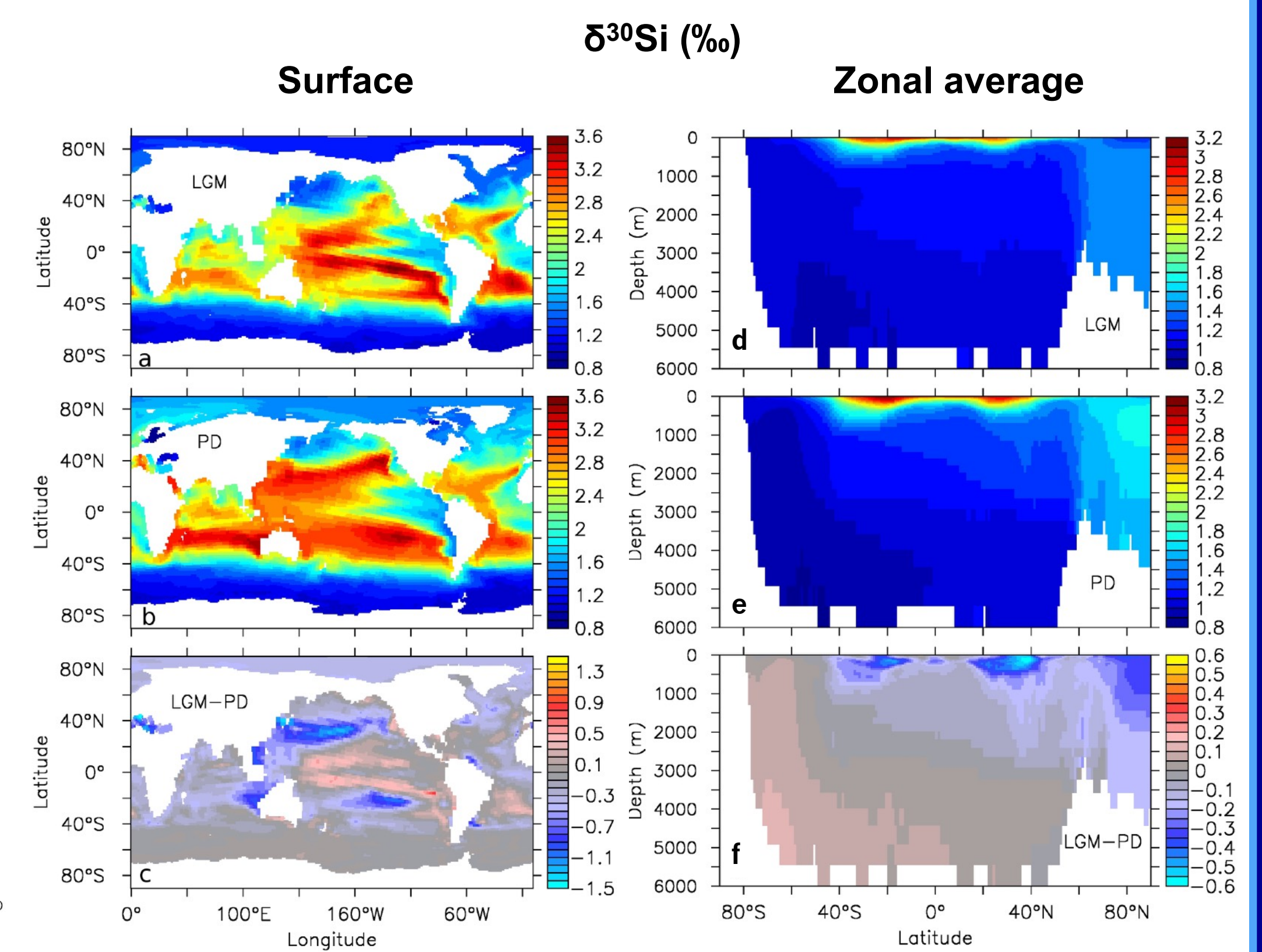
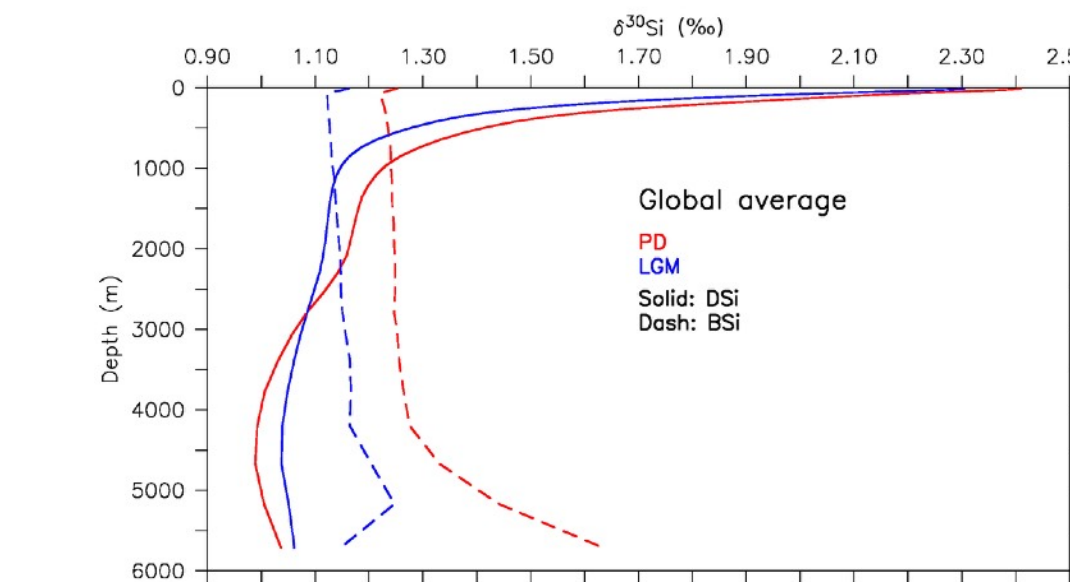
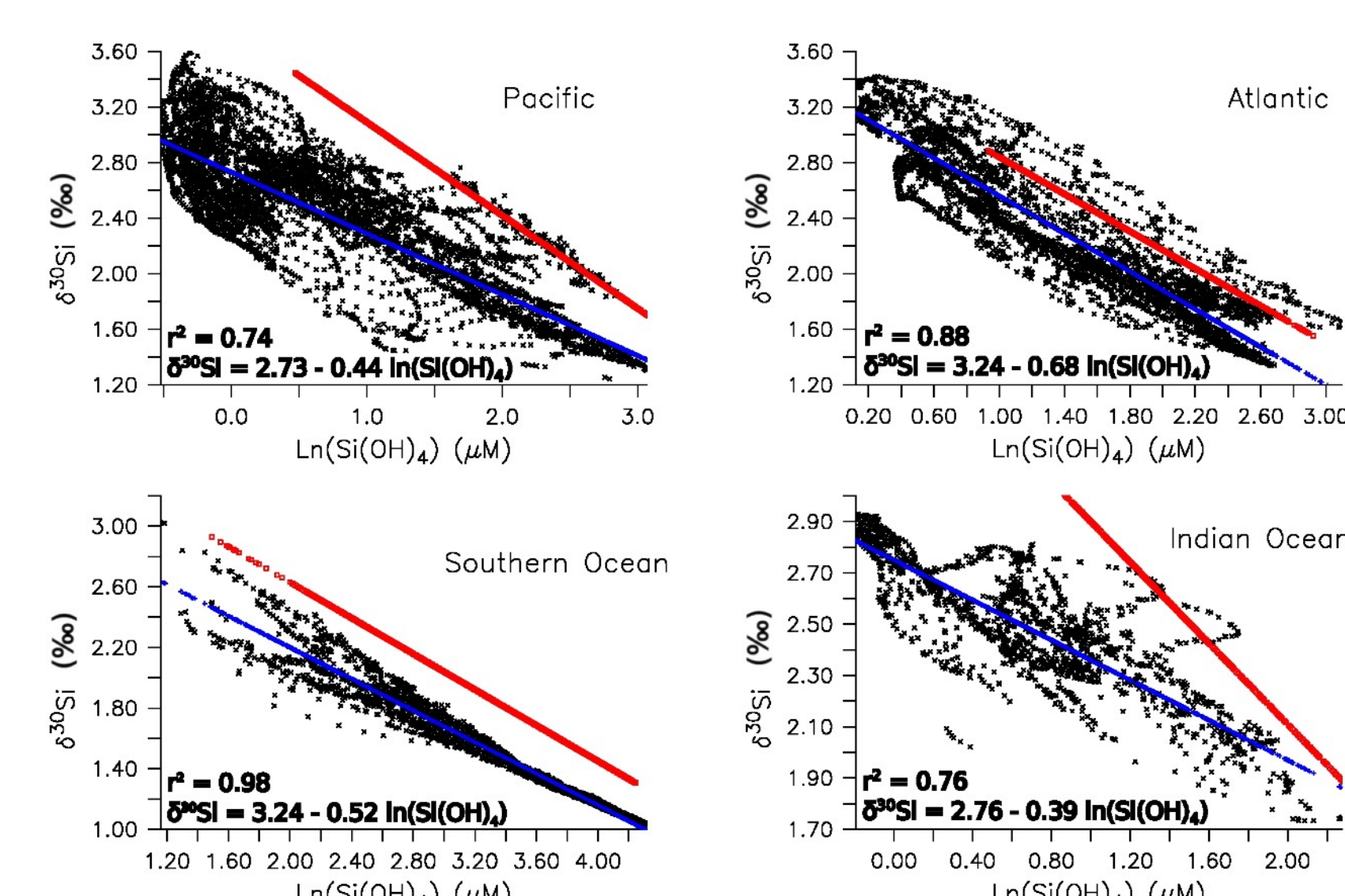


Figure 5: (a-c) Annual mean  $\delta^{30}\text{Si}$  (‰) in the upper 90 m water column; (d-f) zonal mean  $\delta^{30}\text{Si}$  (‰). (a)(d) the LGM run, (b)(e) the PD run, (c)(f) difference between the LGM and PD runs.

Figure 6: The horizontally averaged vertical profiles of  $\delta^{30}\text{Si}$  (‰) of silicic acid and of biogenic silica in both LGM and PD model runs.

### 3. Relation between $\text{Si}(\text{OH})_4$ and $\delta^{30}\text{Si}$



		Pacific	Atlantic	Southern Ocean	Indian Ocean
Slope	LGM	-0.44	-0.68	-0.52	-0.39
	PD	-0.67	-0.67	-0.59	-0.79
Intercept	LGM	2.73	3.24	3.24	2.76
	PD	3.76	3.51	3.81	3.69

Figure 7.  $\delta^{30}\text{Si}$  (‰) versus natural logarithm of silicic acid concentration ( $\mu\text{mol L}^{-1}$ ) in the upper 90 m water column in the four ocean basins in the LGM run. The blue lines are the linear regression curves of  $\delta^{30}\text{Si}$  versus  $\ln(\text{Si}(\text{OH})_4)$  from the LGM run, red lines are linear regression curves from the PD run (data points not shown for the PD run).

- Surface  $\delta^{30}\text{Si}_{\text{DSi}}$  in the LGM and PD is approximately linearly related to the natural logarithm of  $\text{Si}(\text{OH})_4$ , but the slope and intercept differ between ocean basins.
- Surface  $\delta^{30}\text{Si}_{\text{DSi}}$  values in the LGM run are shifted toward lower values compared to the PD run (and to the present-day run in Gao et al. 2016) in all oceans.
- In the Pacific and Indian Ocean the slopes of the surface  $\text{Si}(\text{OH})_4 \sim \delta^{30}\text{Si}$  relation vary between LGM and PD. This is probably caused by different mixing and advection regimes, and complicates interpretation of  $\delta^{30}\text{Si}$  as a proxy for  $\text{Si}(\text{OH})_4$  drawdown

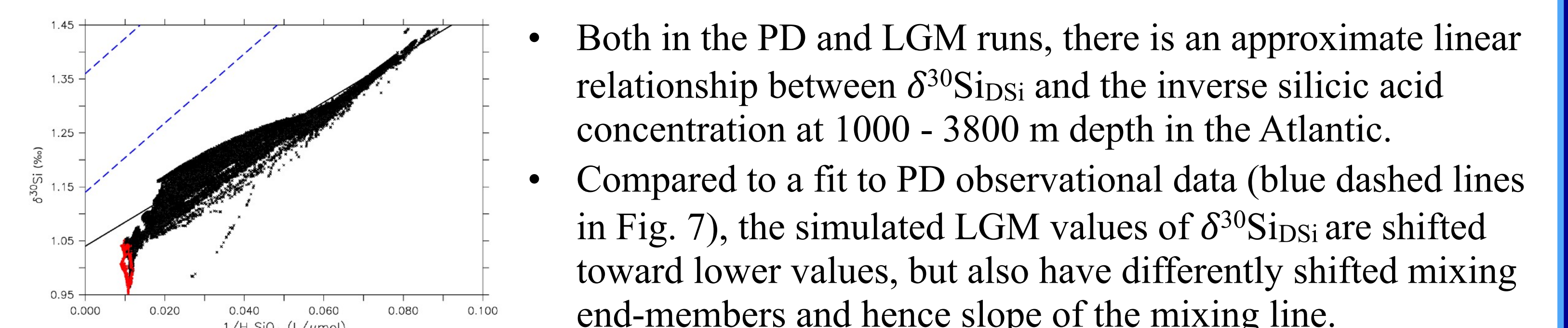


Figure 8. Modeled  $\delta^{30}\text{Si}$  (‰) versus inverse silicic acid concentration ( $\text{L}^{-1}$ ) in the LGM Atlantic (41°S–70°N, 0°W–61°W) below 1000 m depth (scattered crosses in black), with the linear regression (solid black line). The blue dashed lines are linear regressions of the measurements in the Atlantic from Brzezinski and Jones [2015] (the upper line) and de Souza et al. [2012b] (the lower line) (data points are not shown here). Data points in red are between 3800 m and 6000 m, which are not included in the calculation of the regression curve. The PD results are shown in Geo et al., 2016

## Summary and Conclusions

- The mean  $\delta^{30}\text{Si}$  value of DSi in the upper ocean decreases by 0.14‰ in the LGM experiment (river  $\delta^{30}\text{Si}$  has been assumed constant). Values in the low-latitude Pacific increase, caused by an equator-ward shift subtropical gyres, and an increase of equatorial diatom productivity.
- Both surface and deep  $\text{Si}(\text{OH})_4 \sim \delta^{30}\text{Si}$  relations differ between LGM and PD, requiring caution when using sedimentary  $\delta^{30}\text{Si}$  to reconstruct paleo silicic acid utilisation.
- Although our model runs do not take into account an effect of changed Si:N drawdown ratio caused by increased iron supply in the Southern Ocean, our results agree qualitatively with the silicic acid leakage hypothesis.

## References

Zhang, X., Lohmann, G., Knorr, G., and Xu, X. Different ocean states and transient characteristics in Last Glacial Maximum simulations and implications for deglaciation, *Clim. Past*, 9, 2319-2333, <https://doi.org/10.5194/cp-9-2319-2013>, 2013.  
Mark A. Brzezinski, Janice L. Jones (2015), Coupling of the distribution of silicon isotopes to the meridional overturning circulation of the North Atlantic Ocean, *Deep Sea Research Part II: Topical Studies in Oceanography*, 116, 79-88.  
de Souza, G. F., B. C. Reynolds, J. Rickli, M. Frank, M. A. Saito, L. J. A. Gerringa, and B. Bourdon (2012), Southern Ocean control of silicon stable isotope distribution in the deep Atlantic Ocean, *Global Biogeochem. Cycles*, 26, GB2035, [doi:10.1029/2011GB004141](https://doi.org/10.1029/2011GB004141).